VIII International Conference on Computational Methods for Coupled Problems in Science and Engineering
COUPLED PROBLEMS 2019
E. Oñate, M. Papadrakakis and B. Schrefler (Eds)

# TIME REVERSAL METHODS IN ACOUSTO-ELASTODYNAMICS

**Franck Assous*** **and Moshe Lin***

* Department of Mathematics
Ariel University,
Ariel, 40700, Israel.
e-mail: franckassous55@gmail.com
e-mail: moshelin1@walla.co.il

**Key words:** Time Reversal, Elastodynamics, Elastic waves, Wave propagation, Finite Element, Inverse problems

**Abstract.** The aim of the article is to solve an inverse problem in order to determine the presence and some properties of an elastic "inclusion" (an unknown object, characterized by elastic properties discriminant from the surrounding medium) from partial observations of acoustic waves, scattered by the inclusion. The method will require developing techniques based on Time Reversal methods. A finite element method based on variational acousto-elastodynamics formulation will be derived and used to solve to solve the forward, and then, the time reversed problem. A criterion, derived from the reverse time migration framework, is introduced, to help use to construct images of the inclusions to be determined. Our approach will be applied to configurations modeling breast cancer detection, using simulated ultrasound waves.

## 1 INTRODUCTION

Time reversal (TR) is a subject of very active research for over two decades. Many international teams are currently working on the subject from theoretical, physical and numerical points of view. It was originally experimentally developed by M. Fink in 1992 in acoustics and showed very interesting features [1].

Time reversal is a procedure based on the reversibility property of wave propagation phenomena in non-dissipative media. As a consequence, one can "time-reverse" developed signals, by letting them propagate back in time to the location of the source (or scatterers) that emitted them originally. The initial experiment, proposed by M. Fink, was to refocus, very precisely, a recorded signal after passing through a barrier consisting of randomly distributed metal rods. Theoretically, as well as an inverse problem solved in ideal circumstances, TR method should yield the exact solution. However, there is always the possibility that under some (realistic!) conditions, the time reversed process will fail. This may happen due to several reasons: measurement noise, availability of only partial information in space or in time, and lack of knowledge about the medium properties. Since then, numerous applications of this physical principle have been designed, in seismology, for locating the epicenter of an earthquake from measurements taken on the ground [2] and medical imaging [3]. The first mathematical analysis can be found in [4] for a homogeneous medium and in [5], [6] for a random medium.

In a previous Note [16], we have shown the feasibility of a TR method in an acousto-elastic medium. We propose here to extend it by considering more complex acouso-elastic medium that can mimic, for instance, breast tissue configurations. We will apply our approach to identify an "inclusion", or to differentiate between two close inclusions, eventually with different elastic properties, corresponding to different breast tumors, for example, benign and malignant. Indeed, elastic properties of tumor often help to differentiate them: typically, a benign tumor corresponds to normal breast tissues, with a Young modulus between 1 and 70 KPa, whereas malignant tumors have a Young modulus varying from 15 to 500 KPa (see for instance [7]).

## 2 Forward Problem

We first formulate the mathematical forward problem. We consider a two-dimensional fluid-solid domain $\Omega$ made of two parts, an acoustic one $\Omega_f$ and an elastic one $\Omega_s$.

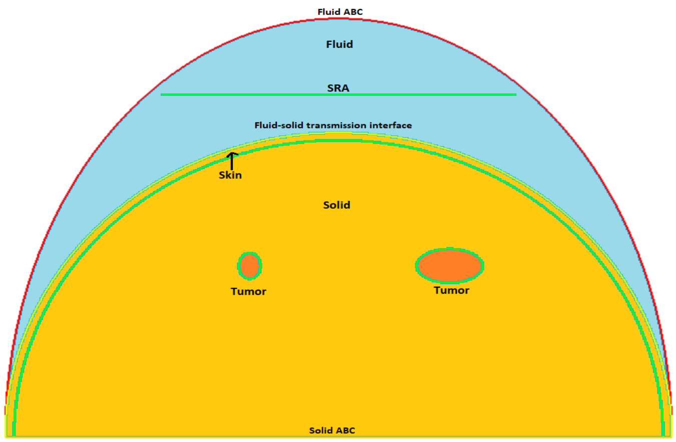


**Figure 1**: Acousto-elastic medium that mimics breast tissue

We will assume that $\Omega$ is half an ellipse (see figure 1). The acoustic part of the domain $\Omega_f$ corresponds to a homogeneous fluid, characterized by its density $\rho_f$ and its Lamé parameter $\lambda_f$. We denote by $\partial\Omega_f$ the boundary of $\Omega_f$ and $\mathbf{n}$ is the outward unit normal to the boundary. Introduce the pressure $p(\mathbf{x}, t)$ on a time $t$, $\mathbf{x} = (x_1, x_2) \in \Omega_f$, and $f(\mathbf{x}, t)$ is a given source, for instance a Ricker function, the acoustic wave equation in $\Omega_f$ is written

$$\frac{1}{\lambda_f}\frac{\partial^2 p}{\partial t^2} - \operatorname{div}\,(\frac{1}{\rho_f}\nabla p) = f\,, \tag{1}$$

together with initial homogeneous conditions. We assume that the boundary $\partial\Omega_f$ can be split into $\partial\Omega_f = \Gamma_f \cup \Gamma_I$, where $\Gamma_I$ denotes the interface between the fluid and solid part, assumed, for simplicity, to be horizontal. We supplement the system with absorbing boundary conditions [15] on $\partial\Omega_f$. Denoting by $V_p = \sqrt{\frac{\lambda}{\rho}}$ the wave velocity in the fluid, the absorbing boundary conditions on $\Gamma_f$ are written

$$\frac{\partial p}{\partial t} + V_p\frac{\partial p}{\partial r} + V_p\frac{p}{2r} = 0 \tag{2}$$

On the part $\Gamma_I$, we add an interface condition for the pressure $p(\mathbf{x}, t)$, that will be presented below, see (5). We then introduce the governing equations of linear elastodynamics for $\Omega_s$, the solid part of the domain, characterized by the density $\rho_s$, and the Lamé parameters $\lambda_s$ and $\mu_s$. We assume that the boundary $\partial\Omega_s$ can be split into $\partial\Omega_s = \Gamma_s \cup \Gamma_I$. Denoting by $\mathbf{u}(\mathbf{x}, t) = (u_1(x_1, x_2, t), u_2(x_1, x_2, t))$ the velocity on a time $t$, at a point $\mathbf{x} = (x_1, x_2) \in \Omega_s$, we have

$$\rho_s\frac{\partial^2 \mathbf{u}}{\partial t^2} - \nabla\cdot(\mu_s\nabla\mathbf{u}) - \nabla((\lambda_s + \mu_s)\nabla\cdot\mathbf{u}) = 0\,, \tag{3}$$

Remark that writing the equation above in terms of velocity (e.g. the time derivative of the displacement) instead of displacement, allows us to derive a pressure-velocity fluid-solid formulation, which will make easier the handling of the transmission conditions during the derivation of the variational formulation, as we will see below.

This equation is supplemented with homogeneous initial conditions and absorbing boundary conditions on $\Gamma_s$, as proposed in [14],

$$\mathbb{A}\frac{\partial \mathbf{u}}{\partial t} = \tau(\mathbf{u})\,\mathbf{n}\,, \tag{4}$$

where the matrix $\mathbb{A}$ is a diagonal $N \times N$ matrix, with $A_{11} = -\sqrt{\rho_s(\lambda_s + 2\mu_s)}, A_{22} = -\sqrt{\rho_s\mu_s}$ for horizontal boundaries, and the contrary for vertical boundaries. A general expression of $\mathbb{A}$ can be found in [14] for more complex geometries of the boundary. Finally, we introduce the transmission conditions at the fluid-solid interface $\Gamma_I$:

$$\frac{1}{\rho_f}\frac{\partial p}{\partial \mathbf{n}} = \frac{\partial \mathbf{u}}{\partial t}\cdot\mathbf{n}\,, \tag{5}$$

$$\frac{\partial p}{\partial t}\mathbf{n} = \tau(\mathbf{u})\,\mathbf{n}\,. \tag{6}$$

These conditions express the continuity of the normal component (5) and of the stress tensor (6) and appear naturally in the pressure-velocity variational formulation, that will be basis of the finite element method. Putting all these equations together, one can derive the following variational formulation in the fluid-solid domain:

$$\begin{aligned}\int_{\Omega_f} \frac{1}{\lambda_f}\frac{\partial^2 p}{\partial t^2} q\, d\omega + \int_{\Omega_f} \frac{1}{\rho_f}\nabla p \cdot \nabla q\, d\omega \\ + \int_{\Gamma_I} \frac{\partial \mathbf{u}}{\partial t}\cdot \mathbf{n}\, q\, d\sigma + \int_{\Gamma_f} (\frac{1}{\lambda_f \rho_f}\frac{\partial p}{\partial t} + \frac{p}{2r\rho_f})\, q\, d\sigma = \int_{\Omega_f} f q\, d\omega\,,\end{aligned} \tag{7}$$

$$\begin{aligned}\int_{\Omega_s} \rho_s \frac{\partial^2 \mathbf{u}}{\partial t^2}\cdot \mathbf{v}\, d\omega + \int_{\Omega_s} \lambda_s \mathrm{div}\,\mathbf{u}\,\mathrm{div}\,\mathbf{v} + 2\mu_s \tau_{ij}(\mathbf{u})\,\tau_{ij}(\mathbf{v})\, d\omega \\ - \int_{\Gamma_I} \frac{\partial p}{\partial t}\mathbf{v}\cdot \mathbf{n}\, d\sigma - \int_{\Gamma_s} \mathbb{A}\frac{\partial \mathbf{u}}{\partial t}\cdot \mathbf{v}\, d\sigma = 0\,.\end{aligned} \tag{8}$$

## 3 Time Reversed Problem

In a second step, we formulate the time reversed acousto-elastic problem. Examples of time reversal techniques, numerical or experimental, can be found (among others) in [1, 9, 10, 11, 12]. We first introduce the time-reversed wave equation for the acoustic part of the domain $\Omega_f$. We denoted by $p^R(\mathbf{x}, t')$ the time-reversed pressure, defined by $p^R(\mathbf{x}, t') = p(\mathbf{x}, T_f - t)$, $\mathbf{x} \in \Omega_f$, where $T_f$ denotes the final time. Since the wave equation involves only second order time derivatives, this definition ensures that the reversed field $p^R(\mathbf{x}, t')$ is a solution to the wave equation

$$\frac{1}{\lambda_f}\frac{\partial^2 p^R}{\partial t'^2} - \mathrm{div}\,(\frac{1}{\rho_f}\nabla p^R) = 0\,, \tag{9}$$

together with (TR) initial conditions and (TR) absorbing boundary conditions on $\Gamma_f$, analogous to (2). In addition, on the boundary $\Gamma_{SRA}$, modeling a source-receivers array (SRA) where the forward signal is recorded (see Fig. 1), we set $p^R(t') = p(T_f - t)$ which is the (recorded) source of the TR.
Similarly, we also introduce the elastic time-reversed problem associated to equation (3). We denote by $\mathbf{u}^R(\mathbf{x}, t') = (u_1^R(x_1, x_2, t'), u_2^R(x_1, x_2, t'))$ the time-reversed velocity solution to linear elastodynamics, that solves

$$\rho_s \frac{\partial^2 \mathbf{u}^R}{\partial t'^2} - \nabla \cdot (\mu_s \nabla \mathbf{u}^R) - \nabla((\lambda_s + \mu_s)\nabla \cdot \mathbf{u}^R) = 0\,, \tag{10}$$

together with (TR) initial conditions and absorbing boundary conditions analogous to (4). Finally, we derive the time-reversed continuity transmission conditions at the interface $\Gamma_I$

$$\frac{1}{\rho_f}\frac{\partial p^R}{\partial \mathbf{n}} = -\frac{\partial \mathbf{u}^R}{\partial t'} \cdot \mathbf{n} \tag{11}$$

$$\frac{\partial p^R}{\partial t'}\mathbf{n} = \tau(\mathbf{u}^R)\,\mathbf{n}\,. \tag{12}$$

Similar to the forward problem, we introduce the time-reversed variational formulation

$$\begin{gathered}\int_{\Omega_f} \frac{1}{\lambda_f}\frac{\partial^2 p^R}{\partial t'^2} q d\omega + \int_{\Omega_f} \frac{1}{\rho_f}\nabla p^R \cdot \nabla q d\omega \\ + \int_{\Gamma_I} \frac{\partial \mathbf{u}^R}{\partial t'} \cdot \mathbf{n} q\, d\sigma + \int_{\Gamma_f} (\frac{1}{\lambda_f \rho_f}\frac{\partial p^R}{\partial t'} + \frac{p^R}{2r\rho_f}) q d\sigma - \int_{\Gamma_{SRA}} f q d\sigma = 0\end{gathered} \tag{13}$$

$$\begin{gathered}\int_{\Omega_s} \rho_s \frac{\partial^2 \mathbf{u}^R}{\partial t'^2} \cdot \mathbf{v}\, d\omega + \int_{\Omega_s} \lambda_s \mathrm{div}\, \mathbf{u}^R\, \mathrm{div}\, \mathbf{v} + 2\mu_s \tau_{ij}(\mathbf{u}^R)\, \tau_{ij}(\mathbf{v})\, d\omega \\ - \int_{\Gamma_I} \frac{\partial p^R}{\partial t'} \mathbf{v} \cdot \mathbf{n}\, d\sigma \, - \int_{\Gamma_s} \mathbb{A} \frac{\partial \mathbf{u}^R}{\partial t'} \cdot \mathbf{v}\, d\sigma = 0\,.\end{gathered} \tag{14}$$

In order to create synthetic data, the forward and reversed formulations are approximated by the FreeFem++ package [13] which implements a finite element method in space. In this study we use a $P_2$ finite element method. The advancement in time is performed by using a second order in time central finite difference scheme, so that it is time reversible also on the numerical level.

## 4 Numerical results

In this section, we describe numerical results obtained for a scatter identification problem, in the case of two scatters located in the elastic part. The principle of the numerical process is as follows: an incident wave is generated by a point source such that after a time $T_f$ the total field is negligible. On the boundary $\Gamma_{SRA}$ located in the fluid part, the forward signal is recorded. Then, we perform numerically a time-reversed computation, by back propagating the recorded scattered data from the SRA. However, we do not assume we know the physical properties or the number of the inclusions, nor their locations. Hence, the recorded data are back propagated in the medium without the inclusions. Finally, we intend to image the unknown scatterers in the medium - responsible of the diffraction of the incident wave - by using correlation method between the forward $\mathbf{u}^I$ and the reversed wave $\mathbf{u}_R^s$ in the same spirit as those involved for instance in time reverse migration [8]. Here, we have considered the following RTM (Reverse Time Migration) criterion:

$$RTM(\mathbf{x}) = \int_0^{T_f} \mathbf{u}_R^s(T_f - t, \mathbf{x}) \times \mathbf{u}^I(t, \mathbf{x}) dt \,. \tag{15}$$

To illustrate our purpose, we consider the medium sketched in Figure 1, made of fluid part (top) and of a elastic one (bottom), the elastic part sketching a breast tissue geometry and is a heterogeneous medium, as it contains a skin layer, i.e. a very thin layer. The SRA is an horizontal line as sketched on Figure 1.

For the fluid part, we choose $\rho = 1000kg/m^3$ and $\lambda = 2.25GPa$, for the solid part, the same value of $\rho$ with $\lambda = 1.83GPa$ and $\mu = 18.33kPa$, and for the skin (inside the solid part), $\rho = 1150kg/m^3$, $\lambda = 6.66GPa$ and $\mu = 66.66kPa$. There are two elliptical inclusions with different size, shape, and elastic properties. The first one represents a benign tumor with $\rho = 1000kg/m^3$, $\lambda = 2.16GPa$ and $\mu = 21.66kPa$, and the second one a malignant tumor, with the same $\rho$, $\lambda = 2.99GPa$ and $\mu = 30kPa$. Note that both inclusions are penetrable, which means that the reflection of the incident wave highlighting the inclusion is quite weak. Finally, the source used to generate the acoustic wave in the fluid part is a Ricker function of the form $f(\mathbf{x}, t) = (1 - 2\pi^2(\nu_0 t - 1)^2)e^{-\pi^2(\nu_0 t - 1)^2}$, with a central frequency $\nu_0 = 100kHz$ and a corresponding wavelength equal to $\lambda_W = 12mm$.

To verify the (in)sensitivity of the method with respect to the noise in the data, we added Gaussian noise to the recorded field $p^S$ with

$$p^S_{Noise} = (1 + \mathit{Coeff} * \mathit{randn}) * p^S$$

where *randn* satisfies a centered reduced normal law and *Coeff* is the noise level, taken equal to 10% in our simulations.

Hence, the scatterers are illuminated by an incident acoustic field, that is first transmitted to the elastic medium through the interface $\Gamma_I$, and then scattered by the inclusions, before to be recorded by the SRA. The SRA being located in the fluid part, they are able to record only a scalar quantity (the pressure $p(\mathbf{x}, t)$), and not a vector velocity $\mathbf{u}(\mathbf{x}, t)$.

However, as shown on images below, where the correlation image between the forward and the reversed wave is depicted (only in the elastic layer), one is able to determine the existence and location of the malignant tumor. The definition of more quantitative criteria to determine the presence and the properties of these inclusions is the subject of our future work.

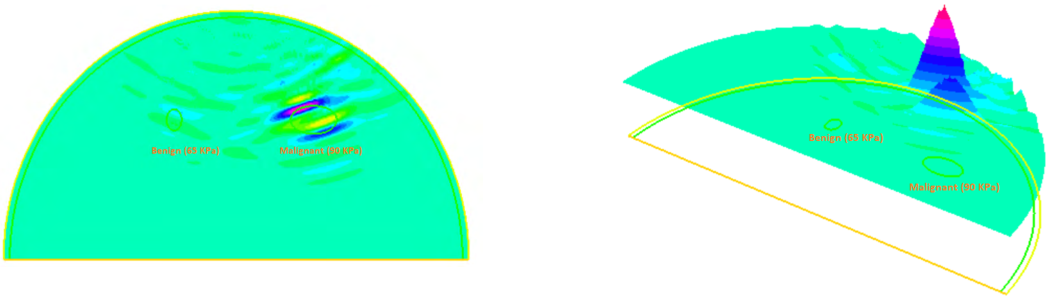


**Figure 2**: Representation of solid part (2D and 3D illustrations)

## 5 Conclusion

We proposed a time-reversal approach for acousto-elastic non homogeneous wave equations. Numerical results have been presented and show satisfactory and promising results in a heterogeneous fluid-solid medium (breast tissue with skin), using only partial information, that is pressure recorded data in the fluid part. By cross-correlating the incident field with the time-reversed scattered field, we were able to determine properties of these inclusions and to differentiate two inclusions, even with different elastic properties. We have now to evaluate quantitatively the obtained elasticity parameters, probably by introducing different cost functions, in the same spirit as what is derived for inverse problems. As usual in this context, optimization based algorithm could be necessary to achieve this part.

## REFERENCES

[1] M. Fink, F. Wu, D. Cassereau, R. Mallart, Imaging through inhomogeneous media using time reversal mirrors. *Ultrasonic Imaging* (1991), **13-2**: 179–199.

[2] C. Larmat, C., J.-P. Montagner, M. Fink, Y. Capdeville, A. Tourin, E. Clévédé, Time-reversal imaging of seismic sources and application to the great sumatra earthquake. *Geophys. Res. Lett.* (2006), *33*: 1–4.

[3] Y. K. Tan, M. Ostergaard, P. G. Conaghan, Imaging tools in rheumatoid arthritis: ultrasound vs magnetic resonance imaging, *Rheumatology*, (2012), **51**: 36–42.

[4] C. Bardos, M. Fink, M. Mathematical foundations of the time reversal mirror. *Asymptot. Anal.* (2002), **29**:157–182.

[5] J.-F. Clouet, J.-P. Fouque, A time-reversal method for an acoustical pulse propagating in randomly layered media. *Wave Motion* (1997), **25**: 361–368.

[6] P. Blomgren, G. Papanicolaou, H. Zhao, Super-resolution in time-reversal acoustics. *J. Acoust. Soc. Am.* (2002), **111**: 230–248.

[7] E. Fernandez, Breast Elastography: Present and Future, *Int. J. Radiol. Radiat. Ther.* (2017), **4(3)**:379–384.

[8] J.F. Claerbout, *Imaging the Earth's interior*. Blackwell, 1985.

[9] F. Assous, M. Kray, F. Nataf, Time-reversed absorbing conditions in the partial aperture case. *Wave Motion* (2012), **49**: 617–631.

[10] F. Assous, M. Kray, F. Nataf, E. Turkel, Time reversed absorbing condition: Application to inverse problems. *Inverse Problems* (2011) ,**27 (6)**: 065003.

[11] P. Kosmas, C.M. Rappaport, Time reversal with the fdtd method for microwave breast cancer detection. *IEEE Transactions on Microwave Theory and Techniques* (2005), **53 (7)**: 2317–2323.

[12] D. Givoli, E. Turkel, Time reversal with partial information for wave refocusing and scatterer identification. *Computer methods in applied mechanics and engineering* (2012), **213-216**: 223–242.

[13] F. Hecht, New development in FreeFem++. *J. Numer. Math.* (2012), **20 (3-4)**: 251–265.

[14] L. Halpern, Etudes des conditions aux limites absorbantes pour des schémas numériques relatifs a des équations hyperboliques linéaires, *Ph.D Thesis*, Paris VI University, 1980.

[15] A. Bayliss, M. Gunzburger, E. Turkel,Boundary conditions for the numerical solution of elliptic equations in exterior regions, *SIAM J. Appl. Math.*, (1982), **42**: 430–451.

[16] F. Assous, M. Lin, Time reversal for obstacle location in elastodynamics from acoustic recording, *Comptes Rendus Mécanique*, (2019).